Geometric Doppler Effect: Spin-Split Dispersion of Thermal Radiation

Nir Dahan, Yuri Gorodetski, Kobi Frischwasser, Vladimir Kleiner, and Erez Hasman*

Micro and Nanooptics Laboratory, Faculty of Mechanical Engineering, and Russell Berrie Nanotechnology Institute, Technion—Israel Institute of Technology, Haifa 32000, Israel

(Received 22 March 2010; revised manuscript received 4 May 2010; published 21 September 2010)

A geometric Doppler effect manifested by a spin-split dispersion relation of thermal radiation is observed. A spin-dependent dispersion splitting was obtained in a structure consisting of a coupled thermal antenna array. The effect is due to a spin-orbit interaction resulting from the dynamics of the surface waves propagating along the structure whose local anisotropy axis is rotated in space. The observation of the spin-symmetry breaking in thermal radiation may be utilized for manipulation of spontaneous or stimulated emission.

DOI: 10.1103/PhysRevLett.105.136402 PACS numbers: 71.36.+c, 42.25.Ja, 44.40.+a, 73.20.Mf

When light is emitted or scattered from a revolving medium, it exhibits a dispersion splitting—angular Doppler effect (ADE)—which depends on the circular polarization handedness (the photon's spin) [1,2]. This splitting is attributed to a spin-dependent correction of the momentum term in the wave equation that results from the transformation to a noninertial reference frame rotating with the medium. The corresponding generalized momentum is the manifestation of the spin-orbit interaction, which is responsible for effects such as the optical spin-Hall [3], Magnus [4], and Coriolis [5] effects, and the Berry phase [6,7]. Here, we report on a geometric Doppler effect manifested by a spin-dependent dispersion splitting of thermal radiation emitted from a structure whose local anisotropy axis is rotated along a certain path in space (superstructure). The observed effect is attributed to modification of the dynamics of the thermally excited surface wave propagating along the superstructure.

Surface electromagnetic waves are confined waves due to the collective oscillations of the free electrons in metal—surface plasmon polaritons—or the resonant collective lattice vibrations in polar crystals—surface phonon polaritons (SPPs). Thermal emission has been shown to be modified by utilizing the high density of states of surface waves and their long-range propagation [8,9]. The coupling of nonradiative surface modes to radiative modes can be achieved by performing a periodic perturbation on the surface, which provides a momentum matching that produces a coherent and polarized emission [8–12]. The radiation dispersion $\omega(k_x)$ of a thermally excited homogeneous silicon carbide (SiC) grating [Fig. 1(a)] is depicted in Fig. 1(b) (measured by Fourier transform infrared interferometer—Bruker-Vertex 70). Here, we investigate the dispersion of structures with reduced symmetry. The first structure is composed of homogeneous grating domains, whose orientation is rotated along the x axis [Fig. 1(c)]. This superstructure is some approximation for a continuous inhomogeneous-anisotropic medium (CIAM) whose local anisotropy axis continuously rotates at angle $\phi(x) = (\pi/a)x$ with a spatial rotation rate $\Omega = d\phi(x)/dx = \pi/a$, where a is the distance along the x axis for the π rotation. The superstructure domains with a local periodicity $\Lambda = 11.6\ \mu$m and a depth of 300 nm were realized using standard photolithographic techniques on a SiC substrate which supports SPPs in the infrared region. The measured dispersions of the superstructures with $a = 240\ \mu$m and $a = 140\ \mu$m, heated to 770 K, are shown in Figs. 1(d) and 1(e). The SPP coherence length in our experiment was measured as $l_c \approx \lambda/\Delta\theta = 73\lambda > 2a$, where $\lambda \approx 12\ \mu$m and $\Delta\theta$ is the angular width of the emission. The resulting picture comprises the zero-order (strong) mode whose dispersion corresponds to the homogeneous structure dispersion split in the momentum dimension according to

$$\omega = \omega(k_x \pm \Omega), \tag{1}$$

and additional (weak) higher-order modes whose origin will be discussed later. Consequently, instead of a single peak at $\omega_0/2\pi c = 833.6\ \mathrm{cm}^{-1}$ (corresponding to $\lambda_0 = 12\ \mu$m) observed in the normal direction $k_x = 0$ [Fig. 2(a), line A], a spectral doublet is measured at $\omega_0 \pm \Delta\omega$, where $\Delta\omega/2\pi c = 8.2\ \mathrm{cm}^{-1}$ [Fig. 2(a), line B], and $\Delta\omega/2\pi c = 14\ \mathrm{cm}^{-1}$ [Fig. 2(a), line C] for the superstructures with $a = 240\ \mu$m and $a = 140\ \mu$m, respectively. According to Eq. (1), for a nearly linear dispersion, the frequency splitting is given by $\Delta\omega = \pm v_x\Omega$, where $v_x = (d\omega/dk)\cos\phi$ is the group velocity of the surface mode in the x direction. This behavior is experimentally observed in Fig. 2(b). Note that, due to the obvious translation symmetry of a superstructure with a period a, the dispersion is expected to be replicated according to

$$\omega = \omega(k_x + mG), \tag{2}$$

where $G = 2\pi/a$ is the superstructure's wave number and m is an integer. Therefore, the observed momentum shift of $\Delta k = \pi/a = G/2$ corresponds to a periodicity of $2a$, which we attribute to the rotational periodicity of the emitted field, and cannot be explained by translation symmetry.

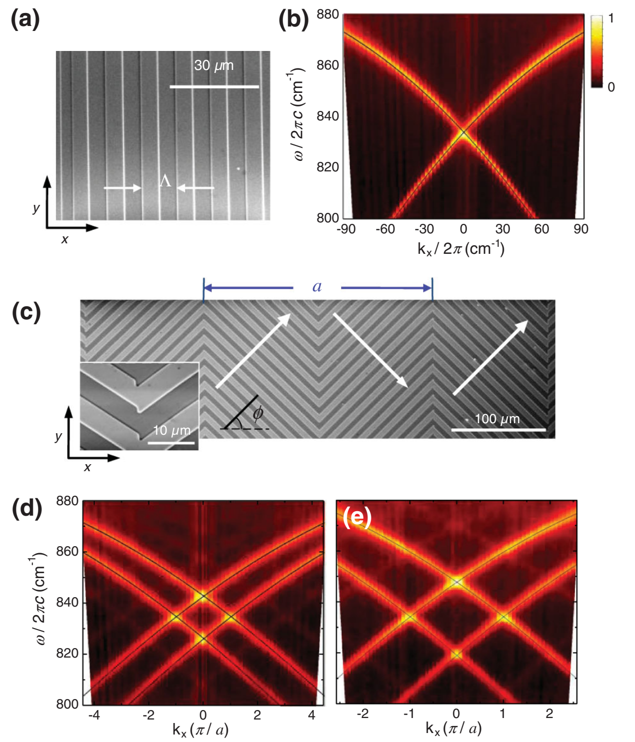

FIG. 1 (color). Dispersion of phonon-polariton superstructures. (a) Scanning electron microscope (SEM) image of the homogeneous grating etched on a SiC substrate with period $\Lambda = 11.6\ \mu$m, depth 300 nm, and filling factor 0.5. (b) Measured dispersion of thermal emission from the homogeneous grating heated to 770 K. Theoretical calculation using the dispersion of SPPs for a flat surface is depicted by solid lines. (c) SEM image of the superstructure composed of two domains oriented at $\pm 45°$; the white arrows depict the local propagation directions of the SPPs in the domains. The inset shows the magnified region of the structure. (d) Dispersion relation measured from the rotating superstructure with period of $a = 240\ \mu$m and (e) $a = 140\ \mu$m. Theoretical calculations [Eq. (1)] are depicted by solid lines. The measured spectral resolution was set to 1 cm^{-1}, the field of view was chosen as 8 mm to avoid edge effects (each sample is 12 mm square), and an angular resolution 0.1°.

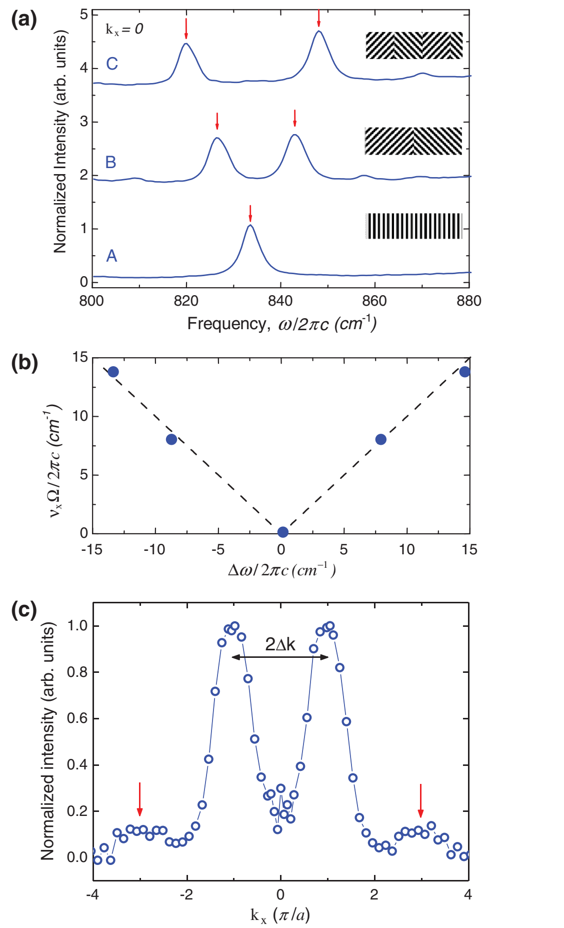

FIG. 2 (color). Doppler splitting of the emission. (a) Emission spectra in normal direction: line A, homogeneous structure; line B, superstructure with period $a = 240\ \mu$m; line C, superstructure with period $a = 140\ \mu$m. (b) Frequency splitting predicted by the ADE (calculated, dashed line; experimental, circles). (c) Emitted intensity versus wave number k_x for the superstructure with period $a = 240\ \mu$m obtained at $\omega_0/2\pi c = 833.6$ cm^{-1}. The red arrows denote the $l_{\pm 3}$ orders, and $\Delta k = \Omega$.

In general, when coherent, polarized light is emitted from a revolving body with angular velocity $\Omega_t = d\phi/dt$, where $\phi(t)$ is the orientation of the body, it will be composed of two modes of opposite circular polarizations. Each mode will be frequency shifted by $\Delta\omega = \sigma\Omega_t$ (to be distinguished from the case of scattering [1] $\Delta\omega = 2\sigma\Omega_t$), where $\sigma = \pm 1$ denotes the spin state associated with right and left circular polarization, respectively [1,2,13,14]. This effect is regarded hereafter as the ADE and provides an explanation for the dispersion splitting observed in our experiment. Although the superstructure is static, the dynamic phenomenon associated with the Doppler effect can be explained by involvement of the propagation of the surface waves. As SPPs travel along the superstructure, they radiate a linearly polarized field that rotates at a spatial rate Ω according to the domain orientation. In addition, the emitted field obtains a phase delay between the domains according to the group velocity of the SPPs in the x direction, v_x. Consequently, the field near the surface can be regarded as a linear polarization rotated along the x direction at a temporal rate $\Omega_t = v_x\Omega$. This situation is most conveniently analyzed from the reference frame attached to the surface mode and rotating according to the local domain orientation. The Helmholtz equation in a noninertial reference frame revolving with rate $c\Omega \ll \omega$ is $(\nabla^2 + k^2 + 2\sigma\Omega k)E_\sigma = 0$, where $E_\sigma = (E_x - i\sigma E_y)/\sqrt{2}$ are the eigenvectors of circular polarizations; note that $2\sigma\Omega k$ is the Coriolis term. This equation can be written as $(\nabla^2 + K^2)E_\sigma = 0$, where $K(\omega) \approx k(\omega) + \sigma\Omega$ is the generalized momentum [2]. A similar term is also obtained in the time-independent Schrödinger equation in the presence of a vector potential [15]. A coupling between the intrinsic and the extrinsic degrees of freedom—spin-orbit interaction—leads to a spin-dependent perturbation of the momentum [3,5–7]. By solving the perturbated Helmholtz equation, we derive the dispersion shift in the momentum dimension,

$$\omega = \omega(k_x + \sigma\Omega). \tag{3}$$

Therefore, due to a rotation of the local anisotropy axis, the original dispersion of the homogeneous structure is now split into two modes with opposite spin states, each shifted by $\Delta k_x = \sigma\Omega$ on the momentum axis. This momentum correction corresponds to the geometric phase shift $\Phi_g(x) = \int \Delta k_x dx = \sigma\phi(x)$, which is the Pancharatnam-Berry phase in the emission process. The derived phase is not a result of optical path differences but arises solely due to local changes in the polarization; note that the geometric phase in the case of scattering was shown to be $\Phi_g(x) = 2\sigma\phi(x)$ [7]. Consequently, the two emitted spin-split modes in the case of CIAM are $E_\sigma \sim \exp(i[k_x(\omega)x + \sigma\phi(x)])(1, i\sigma)^T$, where k_x is the x component of the wave vector of the light emitted from the homogeneous structure, $(1, i\sigma)^T$ is a Jones column vector of circular polarization. However, in the superstructure depicted in Fig. 1(c), the geometric phase distribution corresponds to the stepwise function $F_N\{\phi(x)\}$ with $N = 2$ discrete steps [16,17]. The Fourier expansion of the stepwise function has the form $\exp[iF_N\{\phi(x)\}] = \sum_{l=-\infty}^{\infty} C_l \exp[il\phi(x)]$, where C_l is the lth-order coefficient. For the case of the superstructure with the twin domains ($N = 2$), the two main harmonics $l = \pm 1$ with $|C_{\pm 1}|^2 = 0.405$ give the same contribution; hence, both of the emitted spin-split modes should be degenerated in the momentum domain $E_\sigma \sim \exp[ik_x(\omega)x]\{\exp[i\phi(x)] + \exp[-i\phi(x)]\}(1, i\sigma)^T$. Therefore, we do not expect to observe a pure circular polarization of the emitted light for $N = 2$. This was experimentally confirmed using a polarization analysis by measuring the Stokes parameters. The emission from the superstructure was found to be unpolarized [the degree of polarization was measured as 0.07 compared to 0.86 for TM-polarized emission observed from the homogeneous structure [Fig. 1(a)]]. The reason for this is that the two thermally excited modes are incoherent. To conclude, the Doppler-split dispersion of thermal emission shown in Figs. 1(d) and 1(e) is attributed to a diffraction from a geometric binary π phase $F_{N=2}\{(\pi/a)x\}$ having periodicity of $2a$. Note that the π phase also gives a small amount of diffraction from $l = \pm 3$, $|C_{\pm 3}|^2 = 0.045$, corresponding to a triple spatial rotation rate 3Ω. The additional Doppler-split orders with $\Delta k_x = \pm 3\Omega = \pm 3(\pi/a)$, which are almost an order of magnitude weaker than the main components, can be seen in Figs. 1(d) and 2(c).

The Doppler-split dispersion [Eq. (3)] can be observed when surface waves in distinct domains propagate with the same group velocity component in the x direction as obtained in the superstructure comprising twin domains rotated at $\phi = \pm 45°$ [Fig. 1(c)]. We verified this by a superstructure composed of two orthogonal domains oriented parallel and perpendicular to the x axis [18]. As can be seen in Ref. [18], the replicated dispersion arises as a result of the translation symmetry of the superstructure with a period a, as was described in Eq. (2), rather than the Doppler-split dispersion.

When a grating is used as a coupler, the emitted polarization is unavoidably linked to the surface wave propagation direction resulting from the groove orientation. While we also need to ensure a common v_x, which can be implemented only by twin domains, it is impossible to rotate the polarization in a quasicontinuous way ($N > 2$) using this type of coupler. To remedy this, one needs to break the linkage between the polarization of the emitted field and the propagation direction of the surface waves. Recently, an enhanced transmission via an elliptic hole array in a gold film was reported by Gordon *et al.* [19]. The authors showed that the transmitted light was polarized in the direction perpendicular to the main axis of the ellipses rather than the lattice wave vector. Therefore, this type of coupling between the surface waves and the radiative fields is an effective means for breaking the spin degeneracy. A subwavelength 1.2 μm $\times$ 4.8 μm rod array with a periodicity of $\Lambda = 11.6$ μm was etched to a depth of 1 μm on a SiC substrate [Fig. 3(a)]. In Fig. 3(b), we present the measured dispersion of the homogeneous rod array locally oriented at an angle of 30°. The plot consists of a fast mode related to the usual delocalized surface waves, and a slow mode attributed to coupled, localized phonon polaritons. The observed dispersion of the slow mode is periodic in the momentum with $2\pi/\Lambda$ as expected from a tight-binding mechanism [20] of a coupled thermal antenna array. Polarization analysis confirms that the slow mode's polarization in the homogeneous array is mostly linear. By measuring several rod arrays with different local orientation angles, we verified that the polarization direction of the slow mode is perpendicular to the rods' orientation. Next, an array of rods whose orientation was gradually rotated along the x axis was studied [see Fig. 3(c)]. In this case we implemented $N = 6$ discrete steps $F_{N=6}\{(\pi/a)x\}$; note that the strong main order is only $l = 1$, with $|C_1|^2 = 0.91$, which is a good approximation for a CIAM. The measured dispersion comprises the two modes as before. The fast mode appears in its original location; however, the slow mode exhibits a clear splitting in the momentum [Fig. 3(d)]. Furthermore, the spin-projected dispersion was obtained by measuring the S_3 component of the Stokes vector, $S_3 = i(\langle E_x E_y^* \rangle - \langle E_x^* E_y \rangle)$, which represents the circular polarization portion within the emitted light [18]. For normalized fields $S_3 = \pm 1$ corresponds to pure spin states $\sigma = \pm 1$. Since the eigenstates of the rotating structure are spin states, measurement of S_3 is essential to observe the ADE. Indeed, by measuring the dispersion with respect to S_3 [Fig. 3(f)], we found that the slow mode is shifted by $\Delta k = \sigma\Omega$, as predicted by Eq. (3). Note that at the crossing points of the shifted modes S_3 vanishes, as is expected. Figure 3(e) shows a cross section of the intensity at $\theta = -10°$ (the angle with respect to the normal direction), with and without a circular polarizer so as to elucidate the spin-dependent splitting of the slow

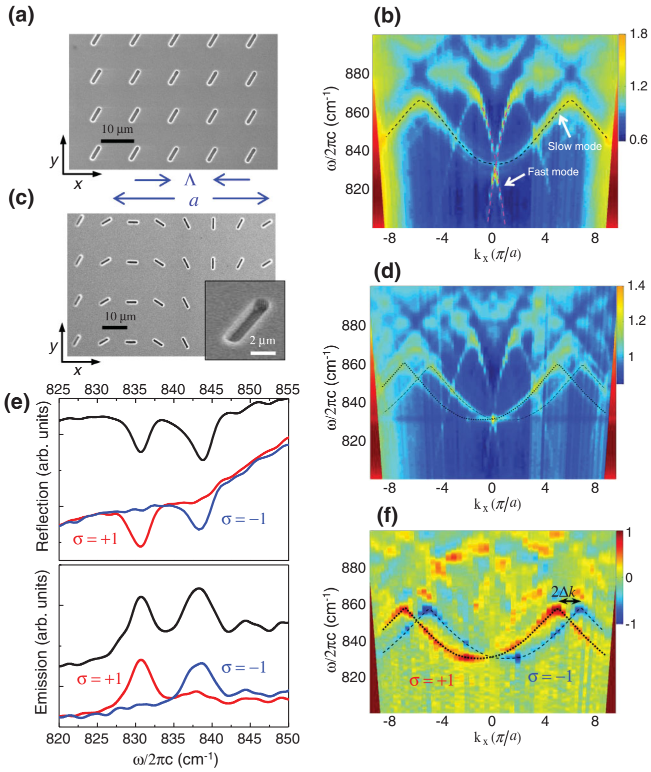

FIG. 3 (color). Dispersion of thermal antenna array. (a) SEM image of the homogeneous rod array with rod dimensions $1.2\ \mu m \times 4.8\ \mu m$, local periodicity of $\Lambda = 11.6\ \mu m$ etched to a depth of $1\ \mu m$ on a SiC substrate. (b) The measured dispersion from rod array depicted in (a). To guide the eye, dashed lines highlight the dispersion of the slow and the fast modes. (c) SEM image of the rod array rotating along the x axis with a period $a = 6\Lambda$. Inset: SEM image of a single rod. (d) Measured dispersion from the rotating rod array. Dashed and dotted black lines indicate the split slow modes. (e) Emission spectrum of the rod array depicted in (c) measured at angle of $\theta = -10°$, and the spectral reflection (illuminated with a thermal source at angle of $\theta = -10°$ and measured at $\theta = 10°$), without a polarizer (black line), with a right-handed circular polarizer (red line), and with a left-handed circular polarizer (blue line); note that the small deviation of the spectral resonances between the emission and reflection is due to temperature effect. (f) Spin-projected dispersion of the rotating rod array, obtained by S_3 measurement. Dashed and dotted lines highlight the dispersion of the spin-split slow mode (red and blue correspond to a positive and negative spin projection, respectively). The obtained dispersion shift is $\Delta k = \sigma\Omega$.

modes. Moreover, from the spectral reflection measurement we verified the spin-dependent absorption of the rotating coupled thermal antenna array [see Fig. 3(e)]. These results support our proposed mechanism of the geometric Doppler effect.

We have demonstrated how spontaneous emission supported by surface waves can be affected by the orientation of the local anisotropy. We experimentally demonstrated spin-dependent dispersion splitting of the emitted light and analyzed it in terms of a geometric Doppler shift. The dispersion splitting due to the spin-orbit coupling is also found as the key feature in such remarkable effects as the Rashba splitting and the spin-Hall effect, which indicates the generic nature of the discussed phenomenon. This may encourage the incorporation of spontaneous or stimulated emission supported by surface waves in the field of spin-optics [5].

This research was supported by the Israel Science Foundation.

*mehasman@tx.technion.ac.il

[1] B. A. Garetz, J. Opt. Soc. Am. **71**, 609 (1981).
[2] S. G. Lipson, Opt. Lett. **15**, 154 (1990); K. Y. Bliokh, J. Opt. A **11**, 094009 (2009).
[3] O. Hosten and P. Kwiat, Science **319**, 787 (2008); K. Y. Bliokh, A. Niv, V. Kleiner, and E. Hasman, Nat. Photon. **2**, 748 (2008).
[4] A. V. Dooghin, N. D. Kundikova, V. S. Liberman, and B. Ya. Zel'dovich, Phys. Rev. A **45**, 8204 (1992).
[5] K. Y. Bliokh, Y. Gorodetski, V. Kleiner, and E. Hasman, Phys. Rev. Lett. **101**, 030404 (2008); Y. Gorodetski, A. Niv, V. Kleiner, and E. Hasman, Phys. Rev. Lett. **101**, 043903 (2008).
[6] M. V. Berry, Proc. R. Soc. A **392**, 45 (1984).
[7] A. Niv, Y. Gorodetski, V. Kleiner, and E. Hasman, Opt. Lett. **33**, 2910 (2008).
[8] J.-J. Greffet, R. Carminati, K. Joulain, J.-P. Mulet, S. Mainguy, and Y. Chen, Nature (London) **416**, 61 (2002).
[9] N. Dahan, A. Niv, G. Biener, Y. Gorodetski, V. Kleiner, and E. Hasman, Phys. Rev. B **76**, 045427 (2007).
[10] T. Setälä, M. Kaivola, and A. T. Friberg, Phys. Rev. Lett. **88**, 123902 (2002).
[11] S. Enoch, G. Tayeb, P. Sabouroux, N. Guérin, and P. A. Vincent, Phys. Rev. Lett. **89**, 213902 (2002).
[12] B. J. Lee and Z. M. Zhang, J. Heat Transfer **129**, 17 (2007).
[13] I. Bialynicki-Birula and Z. Bialynicka-Birula, Phys. Rev. Lett. **78**, 2539 (1997).
[14] V. Bagini, F. Gori, M. Santarsiero, F. Frezza, G. Schettini, and G. Schirripa Spagnolo, Eur. J. Phys. **15**, 71 (1994); R. G. Newburgh and G. V. Borgiotti, Appl. Opt. **14**, 2727 (1975).
[15] M. V. Berry, R. G. Chambers, M. D. Large, C. Upstill, and J. C. Walmsley, Eur. J. Phys. **1**, 154 (1980).
[16] E. Hasman, V. Kleiner, G. Biener, and A. Niv, Appl. Phys. Lett. **82**, 328 (2003).
[17] E. Hasman, Z. Bomzon, A. Niv, G. Biener, and V. Kleiner, Opt. Commun. **209**, 45 (2002).
[18] N. Dahan, Y. Gorodetski, K. Frischwasser, V. Kleiner, and E. Hasman, arXiv:1003.3860.
[19] R. Gordon, A. G. Brolo, A. McKinnon, A. Rajora, B. Leathem, and K. L. Kavanagh, Phys. Rev. Lett. **92**, 037401 (2004).
[20] A. Yariv, Y. Xu, R. K. Lee, and A. Scherer, Opt. Lett. **24**, 711 (1999).